Theory of polariton photoluminescence in arbitrary semiconductor microcavity structures

V. Savona, F. Tassone, C. Piermarocchi, and A. Quattropani
Institut de Physique Théorique, Ecole Polytechnique Fédérale de Lausanne, CH-1015 Lausanne, Switzerland

P. Schwendimann
Defence Procurement and Technology Agency–System Analysis Division, CH-3003 Bern, Switzerland
(Received 1 November 1995; revised manuscript received 30 January 1996)

A quantum theory of quantum well polaritons in semiconductor microcavities is developed. The model takes into account the coupling between the exciton level and the structured continuum of electromagnetic modes relative to the particular geometry of the microcavity. A general equation for the polariton dispersion is obtained as a function of the cavity and exciton parameters. The equation is valid in both weak and strong coupling regimes and reproduces the existing measurements of microcavity polariton dispersion. A model for the polariton luminescence is then derived from the theory. It is possible to define a polariton decay rate only when the resonances in the polariton density of states can be considered as quasimodes. The two limiting cases of very weak and very strong coupling regimes are consequently identified. In these cases the polariton radiative probabilities are derived for light emitted on the left and right sides of the microcavity separately. The influence of the microcavity structure on the polariton dispersion and radiative rates is discussed and in particular the role of the microcavity leaky modes is described in detail. A discussion of the luminescence mechanism in the intermediate coupling case is also presented.

I. INTRODUCTION

Nowadays, the physics of semiconductor microcavities (MC's) has become a widespread research field.[1] In fact, when a quantum well (QW) is placed in a MC, dramatic changes in the intensity of the optical response, the energy of the optical transitions, the radiative lifetimes, and the emission patterns are produced. All these changes appear as a consequence of the strong energy dependence and anisotropy of the optical density inside a MC. Clearly, this density depends on the particular shape of the MC dielectric structure. Therefore a control on the optical response is achieved by tailoring the geometry of the MC. A whole range of possibilities for the design of light-emitting devices is thus opened. In addition, the study of such systems is also interesting from a more fundamental point of view. In fact, the investigation of these modified optical properties in both frequency and time domains allows a better understanding of the dynamics of excitations in confined systems.

Several experiments have been performed in order to characterize these structures. The early works by Weisbuch *et al.*[2] and Yokoyama *et al.*[3] contain experimental evidence of the modified optical response of cavity-embedded QW's. Following these works, several experiments have been performed on MC systems. Houdré *et al.*[4] studied the luminescence of QW excitons in a MC as a function of the emission angle and of the detuning between the exciton energy and the cavity mode. The possibility of varying the detuning by means of an applied electric field or by varying the temperature was proved by Fisher *et al.*[5] Tignon *et al.*[6] have shown the effect of Landau quantization of the carrier free motion by measuring reflectivity spectra under a strong axial magnetic field. Finally, time-resolved measurements[7,8] have been carried out in which the dynamics of the luminescence process has been investigated. A number of theoretical models of the optical properties of QW's in MC's also appeared in the literature. Early theoretical works[9,10] used the Fermi golden rule to calculate radiative recombination rates of excitations in MC's. The golden rule describes the coupling of a discrete level to a continuum in first order perturbation theory.[11] Its validity is limited to the cases when the interaction matrix element between the discrete level and the continuum is small compared to the energy broadening of the continuum density of states. In the MC case the discrete level is the material excitation (QW exciton) and the continuum is constituted by the eigenmodes of the cavity electromagnetic field. Since the density of states of the electromagnetic field in vacuum is flat, the Fermi golden rule works well in the case of a free-standing QW. In MC's this density of states becomes peaked around the cavity resonance. Moreover, the dipole matrix element is proportional to the *local* density of states, defined as the product between the density of states and the normalized amplitude of the electromagnetic field at the QW position. Still, the Fermi golden rule applies if the width of the cavity mode is larger than the interaction matrix element. This situation is called the weak coupling regime. In the opposite case the interaction is no longer described by a purely dissipative process and the Fermi golden rule does not apply. In this strong coupling regime, the decay of the exciton is no longer of exponential nature, and the energy is exchanged between the exciton and the cavity mode several times before being dissipated outside the cavity.

In both cases, the most suitable description of the exciton-radiation interaction in MC's is provided by a polariton formalism. Polaritons are the mixed exciton-radiation states obtained by diagonalizing the total Hamiltonian including the exciton-radiation interaction. Polaritons were first introduced for bulk semiconductors,[12] where the full translational symmetry implies conservation of the wave vector in the exciton-photon interaction. Thus only one photon mode is coupled to

each exciton level. In a QW, beacuse of the breaking of the translational symmetry along the z direction, an exciton level with a given in-plane wave vector $\mathbf{k}_\parallel$ is coupled to the whole continuum of photon modes having the same $\mathbf{k}_\parallel$ and all the possible values of the orthogonal component k_z.[13] Polaritons thus form a continuum which presents resonances in the density of states. In a bare QW, for each exciton level only one resonance appears, whose energy is shifted from the exciton energy by a negligible amount[14] (a few μeV in GaAs). This is the typical situation where the exciton decay process can be described perturbatively, as we have pointed out. When a MC is present, the density of the final radiative states is strongly peaked around the energy of the cavity mode. When this mode is resonant with the exciton level and if the system is in the strong coupling regime, two polariton resonances appear, and the energy shift of each resonance with respect to the exciton dispersion can be up to a few meV. This ''strong'' polariton effect can be explained in close analogy to the case of bulk polaritons. In a MC the electromagnetic field is confined in two dimensions: the energy broadening of the cavity modes is due to the fact that the cavity mirrors are not totally reflecting. When this broadening is small compared to the interaction constant, the exciton interacts with a quasidiscrete two-dimensional (2D) mode and, in a rough approximation, the system behaves like a 2D bulk semiconductor:[15] the polariton splitting is then analogous to that of bulk polaritons. This splitting is usually referred to as vacuum field Rabi splitting, in analogy with atomic physics.[16,17]

The most recent theoretical works on MC's make use of the polariton formalism mainly on two different bases. In the first approach, the system is treated semiclassically:[18,19] Maxwell equations are solved with a nonlocal response function for the QW exciton. The second treatment consists in quantizing the electromagnetic field and diagonalizing the total Hamiltonian of the coupled exciton and radiation fields.[15,20–23] Since the polariton Hamiltonian is quadratic in the two fields, the two treatments give equal dispersion relations for the polariton resonances, as was shown in Ref. 18. However, while the first approach is most suitable for the calculation of reflectivity, transmission, and absorption of a MC system, the second one gives insight into the luminescence process which is closely related to the quantum nature of the polariton states.

The purpose of the present work is to extend the polariton formalism for QW's to the case in which a MC is present. In the first part we present a rigorous quantum mechanical theory of QW exciton polaritons in MC's. The total Hamiltonian including radiation and exciton fields and the polariton interaction is diagonalized. The calculations follow the same steps as in Ref. 20, but the results are extended to the case of an arbitrary asymmetric MC with the QW at arbitrary position inside the cavity body, and to both TE and TM cavity modes. We restrict the calculations to the case where no mixing of the different exciton polarizations is induced by the polariton interaction. The approach here presented extends the formalism introduced in Refs. 15,20–23 to realistic structures with arbitrary dielectric profile and allows one to derive an analytical expression for the polariton dispersion as a function of the exciton and cavity parameters. The model is used to describe the measurements in Ref. 4, and reproduces the experimental data without the use of any adjustable parameter. The second part is devoted to the calculation of the polariton radiative rates in both weak and strong coupling regimes, and to the description of the luminescence process. We show how, in the general case, decay rates for the polariton modes cannot be defined. The validity of the description in terms of decay rates is restricted to the limiting cases of very weak and very strong coupling regimes. A calculation of the polariton radiative rates in these two cases is carried out. It turns out that the main sink of radiation is represented by the so called leaky modes. Leaky modes are cavity modes which originate from the peculiar structure of the distributed Bragg reflectors (DBR's) and radiate in a non-normal direction inside the substrate only. The understanding of this emission mechanism, alternative to that through the main cavity mode, is very important for the design of any MC-based device. One of the advances of this work with respect to the ones cited above is the inclusion of the realistic cavity structure inside the polariton model and, consequently, the detailed description of the influence of leaky modes both on the polariton dispersion and on the radiative rates relative to light emitted at large angles inside the substrate. In Sec. II, the polariton dispersion relation is obtained in an analytical form as a function of the reflection coefficients of the DBR's, the QW position, the exciton dispersion, and the oscillator strength. Then, in Sec. III, the solutions of the dispersion relation are illustrated for some typical cavity structures. In Sec. IV we provide a description of the luminescence process and consider the problem of calculating separately the photon emission probabilities on the air side and inside the substrate. Section V contains a summary and the concluding remarks of the present work.

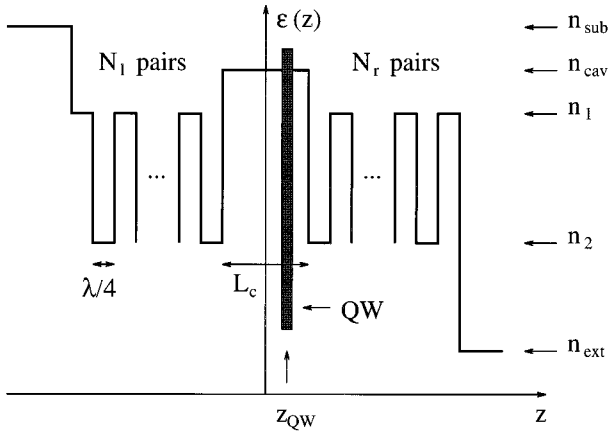

FIG. 1. Plot of the dielectric constant profile of the multilayered structure considered.

II. THEORETICAL MODEL

The system under analysis is depicted in Fig. 1. It is composed of a single QW grown inside a semiconductor MC. A semiconductor MC is a planar Fabry-Pérot resonator where both the central spacer and the two mirrors are made of semiconductor material. In particular, the mirrors, called distributed Bragg reflectors (DBR's), are stacks of semiconductor layers with two alternating refraction indices. We have indicated with N_l and N_r the number of pairs in the left and right

mirrors, respectively. A DBR presents a wavelength interval centered at λ, where $\lambda/4$ is the optical thickness of each semiconductor layer, in which the square modulus of the reflection coefficient at normal incidence is very close to 1, provided the number of pairs is sufficiently high. In addition, the phase of the reflectivity within this region, called the ''stop band,'' behaves linearly as a function of the frequency. The cavity spacer thickness is usually chosen to be an integer multiple of $\lambda/2$. The properties of such a resonator are described in Ref. 24. Here it is important to remark that only a real, frequency independent, dielectric constant is assigned to each layer: no absorption by the MC structure is taken into account. We consider two different refraction indices on the right and left sides of the whole structure because real devices usually have the substrate on one side and air on the other side. The whole structure is planar and a dielectric profile $\epsilon(z)$ is assigned. As shown in Fig. 1, $\epsilon(z)$ is a piecewise constant function; it represents the local background dielectric constant which, inside each semiconductor layer, accounts for the other resonances of the medium. The QW is considered inside the cavity at an arbitrary position z_{QW} with respect to the center of the spacer. In $\epsilon(z)$ we neglect the dielectric mismatch between the cavity and QW materials.

The polariton Hamiltonian is given by

$$H=H_{\mathrm{em}}+H_{\mathrm{exc}}+H_I, \tag{1}$$

where H_{em} and H_{exc} are the noninteracting electromagnetic and exciton Hamiltonians, respectively, and H_I is the standard $\mathbf{A}\cdot\mathbf{p}$ interaction between the electromagnetic and polarization fields.[15] In H_I we neglect the $\mathbf{A}^2$ self-interaction term. This term is important only when we look for the polariton dispersion far from the exciton energy.[15] In order to derive H_{em} and H_I, we need to find the electromagnetic modes of the MC without the QW. The translational symmetry along the plane allows us to write the electric field for a given in-plane wave vector $\mathbf{k}_\parallel$ and frequency ω in the form

$$\mathbf{E}_{\mathbf{k}}(\boldsymbol{\rho},z)=\boldsymbol{\epsilon}_{\mathbf{k}}U_{\mathbf{k}}(z)e^{i\mathbf{k}_\parallel\cdot\boldsymbol{\rho}}. \tag{2}$$

Here $\boldsymbol{\epsilon}_{\mathbf{k}}$ is the polarization vector and $\mathbf{k}=\mathbf{k}_\parallel+k_z\mathbf{z}$. In what follows, we use $k_z=(n_{\mathrm{cav}}^2\omega^2/c^2-k_\parallel^2)^{1/2}$, the z component of the wave vector in the cavity layer, as the continuous index for the cavity modes. Using the previous expression, Maxwell's equations give

$$\frac{d^2U_{\mathbf{k}}(z)}{dz^2}+\left(\frac{\omega^2}{c^2}\epsilon(z)-k_\parallel^2\right)U_{\mathbf{k}}(z)=0. \tag{3}$$

This second order differential equation has two degenerate solutions for each value of k_z and $\mathbf{k}_\parallel$, and for each of the two polarizations. We call these two solutions $U_{j,\mathbf{k}_\parallel,k_z}(z)$ with $j=1,2$. The polarization dependence is not indicated. The solutions of Eq. (3) obey the following orthogonality relation:

$$\int dz\ \epsilon(z)U^*_{j',\mathbf{k}_\parallel,k_z'}(z)U_{j,\mathbf{k}_\parallel,k_z}(z)=2\pi\delta_{jj'}\delta(k_z-k_z'). \tag{4}$$

The orthogonality between $j=1$ and $j=2$ solutions has been imposed in order to write the electromagnetic field in second quantization form. These two solutions are thus determined up to a rotation in the $(j=1,j=2)$ space. The eigenmodes of (3) are propagating modes when ω is larger than $ck_\parallel/n_{\mathrm{sub}}$. This region is usually called the radiative region. Since our aim is to describe the radiative processes, in what follows we restrict ourselves to the radiative region only. When $n_{\mathrm{cav}}>n_{\mathrm{sub}}$, guided modes inside the cavity layer exist for $ck_\parallel/n_{\mathrm{cav}}<\omega<ck_\parallel/n_{\mathrm{sub}}$. These modes, however, are completely confined and, in ideal planar devices, do not contribute to the radiative processes. Actually, guided modes inside the QW layer would appear due to the fact that usually $n_{\mathrm{QW}}>n_{\mathrm{cav}}$. Having neglected the dielectric mismatch (we take $n_{\mathrm{QW}}=n_{\mathrm{cav}}$), these latter modes do not appear in our model. It is known[25] that the coupling to these modes does not introduce important effects inside the radiative region. Once the electromagnetic modes of the cavity are known, the three Hamiltonians can be written in analogy to the derivation of Ref. 15. They read

$$H_{\mathrm{em}}=\sum_{j=1,2}\sum_{\mathbf{k}_\parallel}\int_0^\infty dk_z\ \hbar v(k_\parallel^2+k_z^2)^{1/2}a^\dagger_{j,\mathbf{k}_\parallel,k_z}a_{j,\mathbf{k}_\parallel,k_z}, \tag{5}$$

$$H_{\mathrm{exc}}=\sum_{\mathbf{k}_\parallel}\hbar\omega_{\mathbf{k}_\parallel}A^\dagger_{\mathbf{k}_\parallel}A_{\mathbf{k}_\parallel}, \tag{6}$$

and

$$H_I=\sum_{j=1,2}\sum_{\mathbf{k}_\parallel}\int_0^\infty dk_z\ iC_{j,\mathbf{k}_\parallel,k_z}(a_{j,\mathbf{k}_\parallel,k_z}+a^\dagger_{j,-\mathbf{k}_\parallel,k_z})\times(A_{-\mathbf{k}_\parallel}-A^\dagger_{\mathbf{k}_\parallel}). \tag{7}$$

In these Hamiltonians, $a^\dagger_{j,\mathbf{k}_\parallel,k_z}$ is the creation operator of a photon with given j, $\mathbf{k}_\parallel$, and k_z, $A^\dagger_{\mathbf{k}_\parallel}$ is the creation operator of an exciton with a given $\mathbf{k}_\parallel$, $\omega_{\mathbf{k}_\parallel}$ is the exciton dispersion, and $v=c/n_{\mathrm{cav}}$. It is clear from (7) that the in-plane wave vector $\mathbf{k}_\parallel$ is conserved in the exciton-radiation interaction. The $\mathbf{k}_\parallel$ vector has been discretized, while the k_z component is varied on a continuous range from 0 to $+\infty$. The interaction coefficient in (7) is given by

$$C_{j,\mathbf{k}_\parallel,k_z}=\frac{\omega_{\mathbf{k}_\parallel}}{c}\sqrt{\frac{\hbar v}{(k_\parallel^2+k_z^2)^{1/2}}}F(0)\boldsymbol{\epsilon}_{\mathbf{k}}\cdot\boldsymbol{\mu}_{cv}\times\int dz\ U_{j,\mathbf{k}_\parallel,k_z}(z)\rho(z). \tag{8}$$

Here $F(\boldsymbol{\rho})$ is the exciton envelope function in the QW plane, $\boldsymbol{\mu}_{cv}$ is the dipole matrix element between conduction and valence bands, and $\rho(z)=v(z)c(z)$ is the exciton confinement function.[26] We point out that we have neglected polarization indices in both exciton and photon operators. We are thus considering materials where the polariton interaction does not introduce any polarization mixing and the Hamiltonians for the two polarizations are separated. This situation is typical of heavy hole excitons in GaAs-based materials, where TE modes couple only to the T exciton and TM modes couple only to the L exciton.[14] The extension to light hole Z-polarized excitons has been considered, in the case of a symmetric cavity with metallic mirrors, in Ref. 21. Keeping in mind that this twofold multiplicity exists, we introduce the

polarization dependence only once we have an explicit expression for the polariton dispersion.

We use the Green's function formalism for the diagonalization of the total Hamiltonian. The retarded exciton Green's function is defined as the Fourier transform of the probability amplitude $P_{\mathbf{k}_\parallel}(t)=i\langle 0|A_{\mathbf{k}_\parallel}G_+(t)A^\dagger_{\mathbf{k}_\parallel}|0\rangle$, where $G_+(t)$ is the time evolution operator for $t>0$. The quantity $|P_{\mathbf{k}_\parallel}(t)|^2$ represents the probability that an initial exciton state has not decayed into photons at time t.[11] The retarded Green's function is given by

$$G^{(\mathrm{ret})}_{\mathbf{k}_\parallel}(E)=\frac{1}{E-\hbar\omega_{\mathbf{k}_\parallel}-\hbar\Sigma^{(\mathrm{ret})}_{\mathbf{k}_\parallel}(E)}, \tag{9}$$

where the retarded exciton self-energy is defined as

$$\hbar\Sigma^{(\mathrm{ret})}_{\mathbf{k}_\parallel}(E)=\lim_{\delta\to 0}\sum_{j=1,2}\int_0^\infty dk_z\frac{|C_{j,\mathbf{k}_\parallel,k_z}|^2\hbar v(k_\parallel^2+k_z^2)^{1/2}}{(E-i\delta)^2-\hbar^2v^2(k_\parallel^2+k_z^2)}. \tag{10}$$

These two expressions derive from the standard Green's function formalism[27] and have been used in the framework of the polariton formalism both in bare QW's (Ref. 13) and MC's.[21,22] From the diagonalization of (1) we obtain polariton eigenstates for every value of ω and $\mathbf{k}_\parallel$ in the radiative region. The density of states of this continuum presents peaks which correspond to the polariton resonances. The energy position and broadening of these peaks are given by the real and imaginary parts of the poles of (9) in the complex energy plane.[15,28] The polariton dispersion is defined as the real and imaginary parts of the polariton resonances as a function of $k_\parallel$. The polariton resonances are closely related to the luminescence process, as we will point out in Sec. IV.

A closed form for the exciton self-energy is obtained by replacing (8) into (10):

$$\Sigma^{(\mathrm{ret})}_{\mathbf{k}_\parallel}(E)=\frac{\Gamma_0 k_0}{\pi}\int dz\,dz'\rho(z)\rho(z')G_\xi(z,z'), \tag{11}$$

where $k_0=\omega_0/v$, $\xi^2=E^2/(\hbar^2v^2)-k_\parallel^2$, and

$$G_\xi(z,z')=\lim_{\delta\to 0}\sum_{j=1,2}\int_0^\infty dk_z\frac{U^*_{j,\mathbf{k}_\parallel,k_z}(z')U_{j,\mathbf{k}_\parallel,k_z}(z)}{(\xi-i\delta)^2-k_z^2} \tag{12}$$

is the retarded Green's function of the Maxwell equation (3), expressed as a series development in terms of its eigenmodes. In Eq. (11)

$$\Gamma_0=\frac{2\pi}{n_{\mathrm{cav}}}\frac{\omega_0}{c}\frac{|F(0)|^2|\boldsymbol{\mu}_{cv}\cdot\boldsymbol{\epsilon}_{\mathbf{k}}|^2}{\hbar} \tag{13}$$

is the bare QW exciton radiative rate at $\mathbf{k}_\parallel=0$.[26] Since Eq. (3) defines a Sturm-Liouville problem, Eq. (12) can be rewritten as[27]

$$G_\xi(z,z')=-\frac{2\pi}{\Delta(U_{1,\mathbf{k}_\parallel,\xi}(z),U_{2,\mathbf{k}_\parallel,\xi}(z))}\times\begin{cases}U_{1,\mathbf{k}_\parallel,\xi}(z)U_{2,\mathbf{k}_\parallel,\xi}(z'), & z\leqslant z'\\ U_{2,\mathbf{k}_\parallel,\xi}(z)U_{1,\mathbf{k}_\parallel,\xi}(z'), & z\geqslant z',\end{cases} \tag{14}$$

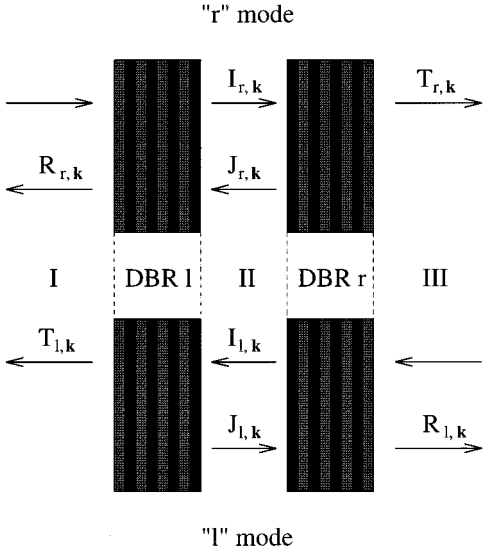

FIG. 2. A sketch of the modes r and l defined in the text. Regions I, II, and III correspond to the external space on the left of the MC, the central cavity layer, and the external space on the right of the MC, respectively.

where $\Delta(U_{1,\mathbf{k}_\parallel,\xi}(z),U_{2,\mathbf{k}_\parallel,\xi}(z))$ is the Wronskian between the two solutions. Equation (14) constitutes a very well known result of the Green's function formalism. Nevertheless, it has not yet been introduced in the context of polariton theory. It allows one to avoid the integration over k_z appearing in the expression for the retarded self-energy, thus constituting a powerful tool to diagonalize the polariton problem in planar structures with arbitrary dielectric constant profile. It is important to remark that in Eq. (14) two independent solutions of Maxwell's equations are required which, however, do not need to be orthogonal.[27] This allows us to drop the assumption of orthogonality in the index j and to choose a convenient form for the two modes. In Eq. (14) and in those which follow we use, instead of the two orthogonal solutions $U_{1,\mathbf{k}_\parallel,k_z}(z)$ and $U_{2,\mathbf{k}_\parallel,k_z}(z)$, two linear combinations $U_{j,\mathbf{k}_\parallel,k_z}(z)$, with $j=l,r$. They are defined as the modes originating from a plane wave traveling from $z=+\infty,-\infty$ respectively, as in Fig. 2:

$$U_{r,\mathbf{k}_\parallel,k_z}(z)=\sqrt{\frac{k_z}{n^2_{\mathrm{cav}}k'_z}}\times\begin{cases}e^{ik'_zz}+R_{r,\mathbf{k}}e^{-ik'_zz}, & z\in\mathrm{I}\\ I_{r,\mathbf{k}}e^{ik_zz}+J_{r,\mathbf{k}}e^{-ik_zz}, & z\in\mathrm{II}\\ T_{r,\mathbf{k}}e^{ik''_zz}, & z\in\mathrm{III},\end{cases} \tag{15}$$

$$U_{l,\mathbf{k}_\parallel,k_z}(z)=\sqrt{\frac{k_z}{n^2_{\mathrm{cav}}k''_z}}\times\begin{cases}T_{l,\mathbf{k}}e^{-ik'_zz}, & z\in\mathrm{I}\\ I_{l,\mathbf{k}}e^{-ik_zz}+J_{l,\mathbf{k}}e^{ik_zz}, & z\in\mathrm{II}\\ e^{-ik''_zz}+R_{l,\mathbf{k}}e^{ik''_zz}, & z\in\mathrm{III}.\end{cases} \tag{16}$$

Regions I, II, and III are defined in Fig. 2, $k'^2_z=(\omega^2/c^2)n^2_{\mathrm{sub}}-k_\parallel^2$, and $k''^2_z=(\omega^2/c^2)n^2_{\mathrm{ext}}-k_\parallel^2$. This choice of modes is the most convenient for treating planar MC's.[21] We further define $r_{j,\mathbf{k}}$ and $t_{j,\mathbf{k}}$, with $j=l,r$ as the complex reflection and transmission coefficients of the left

and right mirror, respectively, for light coming from region II. The coefficients in Eq. (15) can then be calculated, by imposing the boundary conditions on the mirrors, as

$$I_{r,\mathbf{k}}=\frac{k_z'}{k_z}\frac{t_{l,\mathbf{k}}e^{i(k_z-k_z')L_c/2}}{1-r_{l,\mathbf{k}}r_{r,\mathbf{k}}e^{2ik_zL_c}},\quad J_{r,\mathbf{k}}=r_{r,\mathbf{k}}I_{r,\mathbf{k}}e^{ik_zL_c}, \tag{17}$$

$$I_{l,\mathbf{k}}=\frac{k_z''}{k_z}\frac{t_{r,\mathbf{k}}e^{i(k_z-k_z'')L_c/2}}{1-r_{l,\mathbf{k}}r_{r,\mathbf{k}}e^{2ik_zL_c}},\quad J_{l,\mathbf{k}}=r_{l,\mathbf{k}}I_{l,\mathbf{k}}e^{ik_zL_c}. \tag{18}$$

We do not give the expressions for $R_{j,\mathbf{k}}$ and $T_{j,\mathbf{k}}$. In fact, we are interested only in the expression for $U_{j,\mathbf{k}_\parallel,k_z}(z)$ inside the cavity because $\rho(z)$, appearing in (11), is different from zero only in the QW region. It is important to keep in mind that the mirror coefficients $r_{j,\mathbf{k}}$ and $t_{j,\mathbf{k}}$ depend on the polarization. Modes (15) and (16) obey the normalization relation

$$\int dz\ \epsilon(z)U^*_{j,\mathbf{k}_\parallel,k_z'}(z)U_{j,\mathbf{k}_\parallel,k_z}(z)=2\pi\delta(k_z-k_z'). \tag{19}$$

However, it can be verified that, for a given k_z, the two modes $U_{r,\mathbf{k}_\parallel,k_z}(z)$ and $U_{l,\mathbf{k}_\parallel,k_z}(z)$ are not orthogonal to each other. We also define the functions $U_{j,\mathbf{k}_\parallel,\omega}(z)=[\omega/(k_zv^2)]^{1/2}U_{j,\mathbf{k}_\parallel,k_z}(z)$, which obey an orthogonality relation analogous to (19) but with $\delta(\omega-\omega')$ in place of $\delta(k_z-k_z')$. These latter functions will be used in Sec. IV. We can finally replace (17) and (18) into (14) and obtain a closed form for the polariton dispersion as a function of the mirror coefficients:

$$\begin{aligned}&E-\hbar\omega_{\mathbf{k}_\parallel}+2\hbar\Gamma_\alpha k_zP(k_z)\\&\quad+i\hbar\Gamma_\alpha\Bigg[\frac{(1+r_{l,\mathbf{k}}e^{ik_zL_c})(1+r_{r,\mathbf{k}}e^{ik_zL_c})}{1-r_{l,\mathbf{k}}r_{r,\mathbf{k}}e^{2ik_zL_c}}Q^2(k_z)\\&\quad+\frac{(1-r_{l,\mathbf{k}}e^{ik_zL_c})(1-r_{r,\mathbf{k}}e^{ik_zL_c})}{1-r_{l,\mathbf{k}}r_{r,\mathbf{k}}e^{2ik_zL_c}}R^2(k_z)\\&\quad+\frac{2i(r_{l,\mathbf{k}}-r_{r,\mathbf{k}})e^{ik_zL_c}}{1-r_{l,\mathbf{k}}r_{r,\mathbf{k}}e^{2ik_zL_c}}Q(k_z)R(k_z)\Bigg]=0.\end{aligned} \tag{20}$$

Here, α runs over the two polarizations, $\Gamma_{\mathrm{TE}}=\Gamma_0k_0/k_z$ and $\Gamma_{\mathrm{TM}}=\Gamma_0k_z/k_0$. The definitions of functions $P(k_z)$, $Q(k_z)$, and $R(k_z)$ are given, in complete analogy with those by Tassone *et al.*,[29] by

$$P(k_z)=-\frac{1}{2k_z}\int_{z_{\mathrm{QW}}-L/2}^{z_{\mathrm{QW}}+L/2}dz\ dz'\rho(z)\rho(z')\sin(k_z|z-z'|), \tag{21}$$

$$Q(k_z)=\int_{z_{\mathrm{QW}}-L/2}^{z_{\mathrm{QW}}+L/2}dz\ \rho(z)\cos(k_zz), \tag{22}$$

and

$$R(k_z)=\int_{z_{\mathrm{QW}}-L/2}^{z_{\mathrm{QW}}+L/2}dz\ \rho(z)\sin(k_zz), \tag{23}$$

where L is the QW thickness.

III. RESULTS AND COMPARISON WITH EXPERIMENTAL DATA

The dispersion relation derived in the previous section can be solved on the complex energy plane as a function of $\mathbf{k}_\parallel$ and of the exciton and cavity parameters. First, however, we remark that, by letting $r_{j,\mathbf{k}}=0$ and $z_{\mathrm{QW}}=0$ in Eq. (20), the polariton dispersion[29] for heavy hole (HH) excitons in a bare QW is recovered, as expected. A further remark concerns the quantities $P(k_z)$, $Q(k_z)$, and $R(k_z)$. The term proportional to $P(k_z)$ is equal to the one which appears in the QW polariton dispersion[29] and is known to introduce a very small energy shift in the radiative region. We neglect this contribution in the calculations which follow. In the evaluation of $Q(k_z)$ and $R(k_z)$, when $L\ll L_c$ it is possible to replace $\rho(z)$ by a Dirac delta function $\delta(z-z_{\mathrm{QW}})$. We thus take $Q(k_z)=\cos(k_zz_{\mathrm{QW}})$ and $R(k_z)=\sin(k_zz_{\mathrm{QW}})$. Under these approximations, in the case of a symmetric cavity and $z_{\mathrm{QW}}=0$, the results of Refs. 18 and 20 follow from Eq. (20).

In order to illustrate the behavior of the MC polariton dispersion, we solve Eq. (20) numerically for a realistic structure like that in Fig. 1. We point out that, apart from neglecting the term proportional to $P(k_z)$ and introducing the approximations mentioned above for the functions $Q(k_z)$ and $R(k_z)$, we solve Eq. (20) without any pole approximation. In particular, the complex coefficients $r_{j,\mathbf{k}}$ for complex $\mathbf{k}$ values are calculated using a transfer matrix approach.[24] The parameters used for the calculation are the following: $L_c=\lambda$, $N_l=20$, $N_r=14$, $n_{\mathrm{sub}}=3.5$, $n_{\mathrm{ext}}=1$, $n_1=3.35$, $n_2=3.01$, $n_{\mathrm{cav}}=3.0$, and $z_{\mathrm{QW}}=0$. We consider a 75 Å GaAs QW with an exciton energy $\hbar\omega_0=1.59$ eV. For this QW, a realistic value of the exciton radiative rate is $\hbar\Gamma_0=32\ \mu$eV.[26] The cavity length and the mirrors are chosen so that the cavity mode is resonant with the exciton level at $\mathbf{k}_\parallel=\mathbf{0}$. The solutions of (20) on the complex plane are called $E_{\mathbf{k}_\parallel,n}=\hbar(\omega_{\mathbf{k}_\parallel,n}-i\gamma_{\mathbf{k}_\parallel,n})$, where the index n runs over the different polariton resonances at fixed $\mathbf{k}_\parallel$. The real and imaginary parts of $E_{\mathbf{k}_\parallel,n}$ are plotted as a function of $k_\parallel$ in Figs. 3(a) and 3(b), respectively. From now on we indicate only the dependence on the modulus of $\mathbf{k}_\parallel$, if not otherwise required, since we have considered an isotropic Hamiltonian. As solutions of (20), two polariton resonances appear for each value of $k_\parallel$. We recall that these two quantities represent the position of the peaks in the polariton density of states and their broadening, respectively. The most natural interpretation of these resonances is that they correspond to effective quantum levels with a radiative decay rate. We refer to these resonances simply as polariton modes. In Sec. IV we will discuss the limits of this interpretation. The two polariton modes present an energy splitting of 3 meV at $k_\parallel=0$; thus the system is in the strong coupling regime. In this resonance region the polariton modes are admixtures of exciton and photon modes with equal weights. Outside the resonance region the two polariton modes approach the dispersion of the exciton and cavity mode, respectively, and correspondingly they become exciton- and photonlike. This behavior is analogous to that of bulk polaritons, as pointed out in the introduction. Figure 3(b) shows that the polariton radiative rates are substantially different from the bare QW case: the radiative rate of the lower branch shows a peak at $k_\parallel=0$, where it is much higher than the rate Γ_0 of the bare

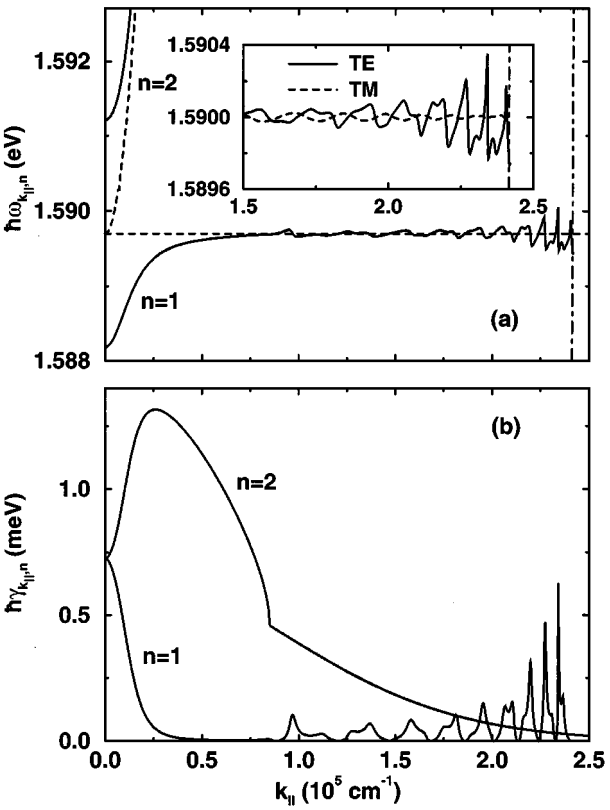

FIG. 3. In graphs (a) and (b), the energy and the radiative rate of the polariton modes are plotted as a function of $k_\parallel$ for TE polarization. The parameters of the structure are described in the text. In plot (a) the dashed lines are the noninteracting exciton and cavity dispersion, while the dashed-dotted line represents the border between radiative and nonradiative regions. The inset in plot (a) shows a detail of the lower polariton dispersion and includes also the TM polarization.

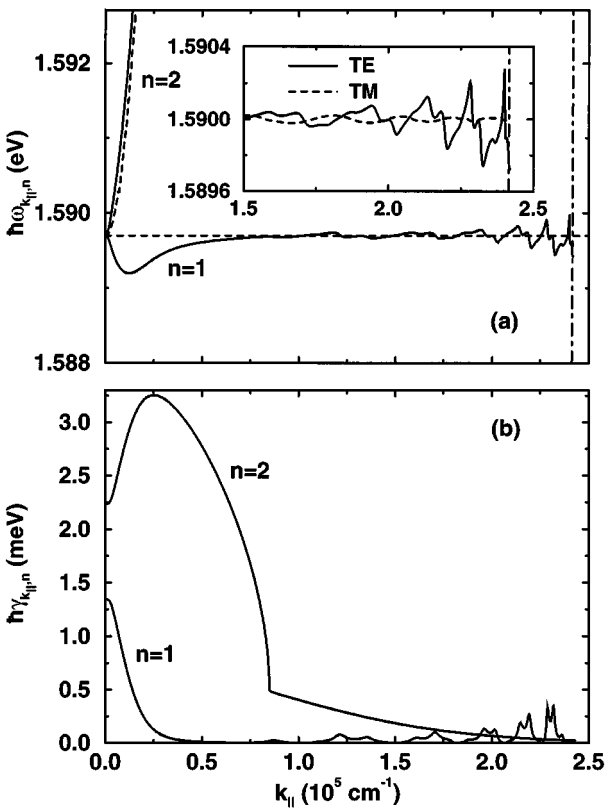

FIG. 4. Same as Fig. 3, but for the weak coupling case described in the text.

QW, and approaches zero at higher values of $k_\parallel$. The peak is a signature of the enhancement of the spontaneous emission due to the resonance with the cavity mode. In the strong coupling regime it can be shown that the radiative rate at resonance is given by one-half of the cavity mode broadening,[18] if no nonradiative exciton broadening is included in the calculation. This result has been known for a long time in atomic physics in the case of strong coupling between a two-level atom and a resonant cavity mode.[17] Out of resonance the lower polariton becomes more excitonlike and consequently its radiative rate lowers to zero. On the contrary, the radiative rate of the upper polariton follows the broadening of the cavity mode and goes to zero as $k_\parallel$ increases. The abrupt change in the slope of the upper polariton rate is due to the onset of total internal reflection on the air side. At larger values of $k_\parallel$ up to k_0, the energy of the lower polariton presents several oscillations, which are shown in detail in the inset of Fig. 3(a). Correspondingly, the radiative rate presents several peaks. These features are due to the coupling of the exciton level to the cavity leaky modes. Leaky modes are electromagnetic modes propagating at finite angles with respect to the growth direction through the DBR into the substrate. They are due to the peculiar structure of the DBR's, which introduces additional resonances in the electromagnetic field at finite angles. The interaction between the exciton and the leaky modes produces an energy shift and an enhancement of the polariton radiative rate, in the same way as for the interaction with the main cavity mode. In Sec. IV we will discuss more in detail the consequences of the interaction with the leaky modes for the emission process.

As a comparison between the weak and the strong coupling cases, we solve again Eq. (20) using the same parameters except for the thickness of the right DBR, for which we choose now $N_r = 8$. The real and imaginary parts of the polariton dispersion are plotted in Fig. 4. Two main differences between Figs. 3 and 4 are evident. First, the Rabi splitting in the polariton energies at $k_\parallel = 0$ has disappeared. Second, the two radiative rates at $k_\parallel = 0$ are now different by a substantial amount. A physical interpretation of these results is the following. In the weak coupling regime the square modulus of the interaction matrix element is smaller than the broadening of the cavity mode. In this situation the exciton level is coupled to an almost flat continuum of photon states. The system presents a full analogy with the bare QW case, the only difference being an increased density of radiative modes at the exciton energy. As a consequence, the two polariton resonances are degenerate at $k_\parallel = 0$. In addition, there is not, as in the strong coupling case, a considerable admixture of exciton and photon modes: in this case one of the two polariton modes is mainly excitonlike and has a smaller radiative broadening, while the other is more photonlike and has a larger broadening. In the limit where the reflectivity of both mirrors vanishes, the broadening of the first polariton approaches Γ_0, while that of the other polariton tends to

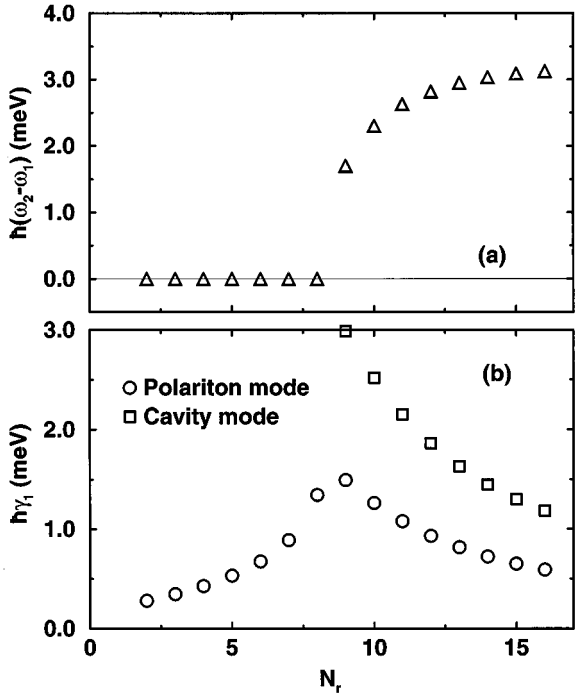

FIG. 5. Plots (a) and (b) represent the polariton (Rabi) splitting and the radiative rate of the lower polariton branch respectively, at $k_{\|}=0$, as a function of the number of pairs of the right hand side mirror, N_r. In plot (b) the energy broadening of the cavity mode is shown for comparison.

infinity, as can be seen from both Eq. (20) and the results of Ref. 18. This limit corresponds, as pointed out at the beginning of this section, to the bare QW case where only one polariton resonance exists.[28] From the comparison between the weak and the strong coupling cases, it comes out that the main difference appears in the resonance region. Here, while in the strong coupling case the two polariton modes are full admixtures of exciton and cavity modes, in the weak coupling case they preserve exciton and photon character, respectively. Outside the resonance region, in both cases, the amount of exciton-photon admixture is negligible.

In order to understand the transition from weak to strong coupling regime, we plot in Fig. 5(a) the Rabi splitting at $k_{\|}=0$ as a function of the number N_r of pairs of the mirror on the air side. In correspondence, Fig. 5(b) shows the radiative rate of the lower polariton mode. For small N_r the system is in the weak coupling regime and no Rabi splitting is present. In the weak coupling regime the polariton radiative rate is the one given by the Fermi golden rule. Increasing the confinement of the radiation, we can clearly see the transition from weak to strong coupling and the onset of a finite Rabi splitting. The broadening of the cavity mode has been plotted for comparison. It is clear from Fig. 5(b) that in the strong coupling regime the polariton radiative rate is equal to one-half of the cavity mode broadening. The radiative rate shows its maximum in the transition from weak to strong coupling. Moreover, the value at the maximum is much larger than Γ_0. This effect is usually called enhancement of the spontaneous emission. For lower N_r, the radiative rate decreases, approaching the value of the bare QW Γ_0, as mentioned above.

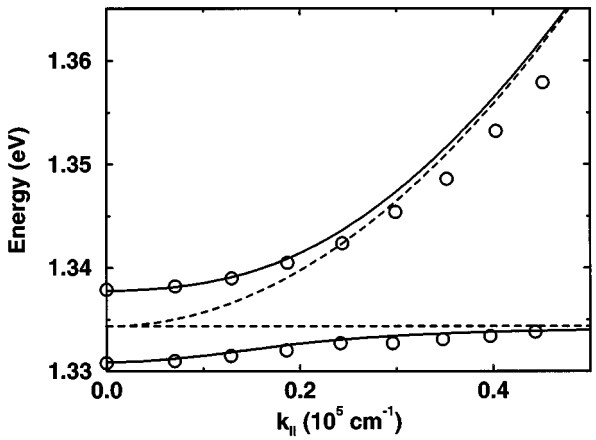

FIG. 6. The comparison between experimental data from Ref. 4 and our calculation. The parameters used in the calculation are given in the text. The dashed lines represent the noninteracting exciton and cavity modes.

As a test of the present model, we show in Fig. 6 the polariton dispersion measured in Ref. 4 and our theoretical prediction. The sample in Ref. 4 consists of a 3/2λ MC with six embedded GaAs/$In_xGa_{1-x}As$ QW's. Our model takes into account one QW only. The most rigorous treatment of the multiple-QW case consists in diagonalizing the coupled problem of the N QW exciton states plus the radiation field, as was shown by Citrin for bare multiple QW's.[30] From this treatment it turns out that only one of the N multiple-QW exciton states gives rise to a radiative polariton, the other $N-1$ states having negligible radiative broadening. In the long wavelength approximation, the radiative state has an oscillator strength equal to N times the single-QW oscillator strength.[21] In a MC, however, this approximation is not very accurate. It turns out from Ref. 30 that a more accurate approximation consists in weighting the oscillator strength of each QW with the square modulus of the normalized electric field amplitude at the QW position. Following this approach, an effective number of QW's, N_{eff}, is derived in Ref. 18. In the present case, $N_{\mathrm{eff}}=5.34$. In the calculation we have used $\hbar\Gamma_0=22$ μeV, which has been obtained from the existing measurements of the exciton oscillator strength in GaAs/$In_xGa_{1-x}As$ QW's.[31] The cavity parameters used for the calculation are those described in Ref. 4 and no fitting procedure was necessary. It can be seen in Fig. 6 that the data are reproduced very well by the present model. The deviation in the upper polariton branch at high $k_{\|}$ values must be attributed to an experimental uncertainty in the measurement of the angle.[32]

Before introducing, in the next section, a description of the luminescence process, we address the problem of including a nonradiative dissipation rate for the exciton. This rate should account for all the possible exciton dephasing mechanisms, like phonon and impurity scattering, radiative traps, surface recombination, etc. A way to take into account the homogeneous broadening of the exciton level is to include an imaginary part in the exciton dispersion appearing in Eq. (20). Once $\omega_{\mathbf{k}_{\|}}$ is replaced by $\omega_{\mathbf{k}_{\|}}-i\gamma_{\mathrm{exc}}$, where γ_{exc} is the nonradiative exciton broadening, the polariton dispersion can be solved for energies on the complex plane, as before. In

this case, however, the imaginary part of the solutions represents the total polariton decay rate, including the direct radiative recombination and the exciton nonradiative dissipation mechanisms. In the general case, the separate calculation of the radiative and nonradiative rates of polariton modes is not a trivial task. In fact, acoustic phonons act both as scattering centers for the coherent polaritons and as a source of phase-coherence loss for exciton states (and consequently for the polariton interaction). Even if these two mechanisms can be included separately in a QW exciton polariton formalism,[33,34] the inclusion of both would require the solution of the three-field problem at finite temperature. This problem, to the authors' knowledge, has never been addressed. In the next section the polariton radiative decay probabilities are calculated in the presence of the nonradiative homogeneous broadening introduced before, under some assumptions (which will be stated later) on the relaxation and dephasing processes, in two general cases.

IV. POLARITON PHOTOLUMINESCENCE

In this section we describe the photoluminescence process of cavity polaritons and show that a simple description in terms of emission rates is possible only in well defined cases. In a photoluminescence experiment, excited states are produced at energies larger than those of the observed signal. The excitations thus created relax towards the lowest energy states which, in our case, are the cavity polaritons. The relaxation takes place through all the different polariton scattering mechanisms. In particular, in high quality samples at low temperature the dominant mechanism is the scattering by acoustic phonons.[33] When the relaxation process brings polaritons inside the radiative region, some of them radiate while the others further relax towards the bottom of the polariton dispersion. Only the radiated signal is observed by external detection. The balance between relaxation and emission processes is determined by the radiative rates at different $k_{\parallel}$ values within the radiative region and the scattering rates between polaritons at different wave vectors. A detailed analysis of the competition between these two effects has been presented elsewhere.[35] Here we just want to remark that points in the radiative region where the radiative rate is much larger than the scattering one will behave as radiative sinks for polaritons. This, in turn, will result in a bottleneck in the relaxation process. We will further consider this mechanism later on in this section, in connection with the discussion of the influence of cavity leaky modes on the radiative process. In general, the complete dynamics of the relaxation and recombination processes has to be computed in order to derive the intensity of the radiated light as a function of time and emission angle. Here, however, we want to consider the luminescence process under continuous excitation. In this particular case the detailed balance principle assures that a stationary polariton distribution will exist. In case relaxation is faster than the recombination rates of the system, this distribution will of course correspond to the thermal one. Otherwise, fast decaying states and bottlenecks in the relaxation will result in a nonthermal, but still stationary, distribution. In bare and in MC-embedded QW's, at temperatures where the scattering on acoustic phonons is the main relaxation mechanism, the second hypothesis is most likely to be verified.[33,35] For this reason, here we assume the polariton distribution as given, regardless of its thermal character, and concentrate on the calculation of the polariton radiative rates as a function of $k_{\parallel}$.

We point out that, in the picture presented above, the states in the radiative region are identified as coherent polariton states. This means that we assumed dephasing effects on the polariton interaction to be negligible. These effects originate from exciton-phonon interactions, exciton-exciton interactions, and interface and alloy disorder. While the first two sources of dephasing can be limited by performing experiments at sufficiently low temperature and excitation density, the effect of disorder is important in any experimental regime.[36] We will discuss at the end of this section the conditions under which the assumption of coherent polariton interaction is justified.

In order to compute the radiative recombination rates, it is necessary to know the initial states of the decay process. We distinguish two cases where the initial state is determined by simple considerations. The first situation is that of the very weak coupling regime between degenerate exciton and cavity modes. In this case, as we have seen, the two polariton resonances are degenerate and one is much broader than the other. The broader resonance is almost completely photonlike while the other is almost completely excitonlike. The very weak coupling is close to the bare QW case: only the narrower of the two polariton resonances is affected by relaxation mechanisms and therefore significant for the optical properties. As a consequence, in the very weak coupling regime, the initial state to calculate a decay rate is the bare exciton state. The second situation arises when $\omega_{k_{\parallel},2}-\omega_{k_{\parallel},1} \gg (\gamma_{k_{\parallel},1}+\gamma_{k_{\parallel},2})/2$, namely, when there is a large splitting and two clearly distinct peaks in the polariton density of states. This situation takes place when the exciton and cavity modes are completely detuned or, in case they are resonant, when the system is in the very strong coupling regime. The structure of the polariton density of states allows us to identify the polariton peaks as quasiparticles in the sense of many-body theory. The natural choice of the initial state of decay in the very strong coupling case is a polariton quasiparticle. This can be explained by introducing a simple picture of the MC polariton quasiparticle, as a superposition of an exciton and the discrete mode of a closed cavity. The decay arises when the weak coupling to the external continuum of radiation is considered. This picture is usually called the quasimode picture.[37] In very strong coupling, the Rabi oscillation, of period $2\pi(\omega_{k_{\parallel},2}-\omega_{k_{\parallel},1})^{-1}$, between the exciton and photon states which constitute the quasimode is presumably much faster than scatterings involved in the relaxation processes. Consequently, the polariton quasimode would be the appropriate initial state. In the following calculation, however, we choose the exciton as the initial state of decay. The exciton itself can be expressed as a superposition of the polariton quasimodes. It will be shown that the two polariton decay rates may be easily extracted from this calculation.

In order to calculate the total radiative rate in the very weak and very strong coupling cases, we choose the appropriate linear superposition of l and r modes, whose electric field is symmetric around the QW position z_{QW}. This mode

is the radiative one, since we assume a symmetric exciton wave function, while the antisymmetric combination clearly does not couple to the exciton. We call this mode $U_{s,\mathbf{k}_\parallel,\omega}(z)$, and $a^\dagger_{s,\mathbf{k}_\parallel,\omega}$ the corresponding photon creation operator. The time dependent probability per unit frequency of an initial exciton decaying into the symmetric mode is defined as

$$\frac{dP_{k_\parallel,\omega}}{d\omega}(t)=|\langle 0|a_{s,\mathbf{k}_\parallel,\omega}G_+(t)A^\dagger_{\mathbf{k}_\parallel}|0\rangle|^2. \tag{24}$$

The matrix element appearing in (24) could in principle be calculated perturbatively. However, in order to obtain the correct time dependent probability in the strong coupling regime it is necessary to go beyond perturbation theory. In the present case, the perturbation series deriving from (24) can be summed exactly[11] and the result, in terms of the interaction matrix element and the retarded Green's function, is given by

$$\langle 0|a_{s,\mathbf{k}_\parallel,\omega}G_+(t)A^\dagger_{\mathbf{k}_\parallel}|0\rangle=\frac{\langle 0|a_{s,\mathbf{k}_\parallel,\omega}H_IA^\dagger_{\mathbf{k}_\parallel}|0\rangle}{2\pi}\times\int dE\,\frac{e^{i(\hbar\omega-E)t/\hbar}}{E-\hbar\omega+i\epsilon}G^{(\mathrm{ret})}_{\mathbf{k}_\parallel}(E), \tag{25}$$

where $G^{(\mathrm{ret})}_{\mathbf{k}_\parallel}(E)$ has been defined in Sec. II. Using (7) we express the matrix element in (25) as

$$\langle 0|a_{s,\mathbf{k}_\parallel,\omega}H_IA^\dagger_{\mathbf{k}_\parallel}|0\rangle=iC_{s,\mathbf{k}_\parallel,\omega}, \tag{26}$$

where the coefficient $C_{s,\mathbf{k}_\parallel,\omega}$ is defined as in (8) with $U_{s,\mathbf{k}_\parallel,\omega}(z)$ in place of $U_{j,\mathbf{k}_\parallel,k_z}(z)$. Equation (25) allows the calculation of the time dependent decay probability in any coupling regime. However, as stated above, we are studying only the two limiting cases of very weak and very strong coupling. In these two cases some approximations can be introduced in order to derive a simple expression for the decay probability. As a first step, Eq. (25) can be integrated on the complex plane. The result is

$$\langle 0|a_{s,\mathbf{k}_\parallel,\omega}G_+(t)A^\dagger_{\mathbf{k}_\parallel}|0\rangle=\frac{iC_{s,\mathbf{k}_\parallel,\omega}}{\hbar}\left[\frac{1}{\omega-\omega_{\mathbf{k}_\parallel}-\Sigma^{(\mathrm{ret})}_{\mathbf{k}_\parallel}(\hbar\omega)}-\sum_{n=1,2}\frac{e^{-i(\omega_{k_\parallel,n}-\omega)t}e^{-\gamma_{k_\parallel,n}t}}{\omega-\omega_{k_\parallel,n}+i\gamma_{k_\parallel,n}}\right], \tag{27}$$

where the second term in square brackets is obtained under the approximation of two simple polariton poles for the Green's function $G^{(\mathrm{ret})}_{\mathbf{k}_\parallel}(E)$.[38] In both very weak and very strong coupling cases, the first term in square brackets can be approximated by a sum over the two simple poles, in analogy to the second term. As explained before, the two polariton modes contribute to the matrix element (27). In very weak coupling, only one mode contributes significantly to the calculation, because the other has a very large broadening. In very strong coupling, instead, the time dependence would involve interference between the two modes. However, as mentioned above, this is a consequence of having chosen the exciton as the initial state of the decay. When only one polariton quasimode is used, only the corresponding term will appear. This allows us to carry out the calculation for each resonance and in both very weak and very strong coupling we finally obtain for $\gamma_{k_\parallel,n}t\ll 1$

$$\frac{dP_{k_\parallel,\omega}}{d\omega}(t)=\frac{|C_{s,\mathbf{k}_\parallel,\omega}|^2}{\hbar^2}\frac{\gamma_{k_\parallel,n}t}{(\omega-\omega_{k_\parallel,n})^2+\gamma^2_{k_\parallel,n}},\quad n=1,2\,. \tag{28}$$

The radiative rate is calculated by taking the time derivative of (28), and integrating over the frequency ω:

$$\gamma^{\mathrm{rad}}_{k_\parallel,n}=\frac{2\pi}{\hbar^2}|C_{s,\mathbf{k}_\parallel,\omega_{k_\parallel,n}-i\gamma_{k_\parallel,n}}|^2. \tag{29}$$

This expression is analogous to the Fermi golden rule, but is calculated on the polariton resonances. The coefficient $C_{j,\mathbf{k}_\parallel,\omega}$ can be evaluated for complex ω using (8), (15), and (16), and extending the calculation of $r_{j,\mathbf{k}}$ and $t_{j,\mathbf{k}}$ to complex values of k_z.

Equation (29) defines the total radiative rate. Actually, in a MC, light with a given $k_\parallel$ can radiate through the two DBR's on both sides of the structure. Moreover, because of the asymmetry of the MC, the probabilities of a photon being emitted through the left mirror inside the substrate and through the right mirror in empty space will in general be different. As a consequence of this asymmetry, a hypothetical time resolved luminescence experiment, performed separately on the two sides of the sample, would result in the same decay time, determined by the total radiative rate calculated above, but different intensities of the measured signal at a given time. As an example, it is clear that for large enough $k_\parallel$, total internal reflection sets in for the mirror on the air side and light is emitted in the substrate only. Since in most of the luminescence experiments luminescence is detected on the air side only, it is necessary to further distinguish a left and a right emission probability in the emission process. In what follows, in order to avoid confusion, we will speak of radiative ''rate'' only in relation to the total radiative rate calculated above, while we will call left and right emission ''probabilities'' the two quantities derived below, even if their derivation closely follows that of the total rate. We remark that modes of type l and r are the appropriate modes to represent a right and left *outgoing* photon, respectively. This becomes evident if the time reversal operator is applied to these two modes, as can be seen from Fig. 2. The derivation of the left and right decay probabilities cannot be carried out as was done for the total rate, because the two modes l and r are not orthogonal. This fact represents the main difference between our case and cases where the standard scattering theory can be applied. We are forced to calculate the decay probability over finite photon wave packets in order to overcome this difficulty. We define our incoming wave packet from the right as

$$\psi^{(\mathrm{in})}_{r,\mathbf{k}_\parallel,\omega}(\mathbf{r},t)=\int d\omega'\,\xi_r(\omega-\omega')U_{r,\mathbf{k}_\parallel,\omega'}(z)e^{i(\mathbf{k}_\parallel\cdot\boldsymbol{\rho}-\omega' t)}. \tag{30}$$

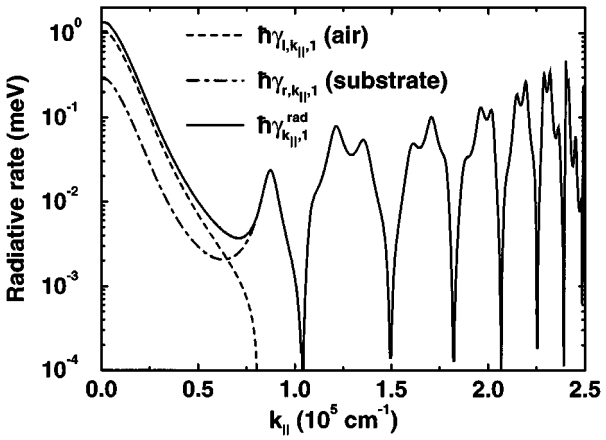

FIG. 7. The total radiative rate and the corresponding emission probabilities for left and right emitted photons are plotted for the structure with $N_r=8$ described in the text.

The wave packet outgoing in the $-\infty$ direction is simply obtained by applying the time reversal operator on the incoming packet as $\psi^{(\mathrm{out})}_{l,\mathbf{k}_{\|},\omega}(\mathbf{r},t)=[\psi^{(\mathrm{in})}_{r,\mathbf{k}_{\|},\omega}(\mathbf{r},t)]^*$. Incoming and outgoing wave packets on the right side are defined in an analogous way using l modes. The calculation of the exciton decay probability into the outgoing packets follows the same steps as for the total radiative rate. If we consider the probability for $\gamma_{k_{\|},n}t\gg 1$, we obtain

$$P_{j,\mathbf{k}_{\|},\omega}=\frac{1}{\hbar^2}\left|\int d\omega'\,\xi_j(\omega-\omega')\frac{C_{j,\mathbf{k}_{\|},\omega'}}{\omega'-\omega_{\mathbf{k}_{\|}}-\Sigma^{(\mathrm{ret})}_{\mathbf{k}_{\|}}(\hbar\omega')}\right|^2, \quad j=l,r. \tag{31}$$

As usual, this expression can be simplified in the two limiting cases of very weak and very strong coupling regimes. The result is again proportional to $|C_{j,\mathbf{k}_{\|},\omega_{k_{\|},n}-i\gamma_{k_{\|},n}}|^2$ and depends on the shape of the wave packet. This latter dependence drops out in the ratio between left and right decay probabilities obtained, as before, by integrating (31) over ω:

$$\frac{P_{l,\mathbf{k}_{\|},n}}{P_{r,\mathbf{k}_{\|},n}}=\frac{|C_{r,\mathbf{k}_{\|},\omega_{k_{\|},n}-i\gamma_{k_{\|},n}}|^2}{|C_{l,\mathbf{k}_{\|},\omega_{k_{\|},n}-i\gamma_{k_{\|},n}}|^2}, \quad n=1,2. \tag{32}$$

The values obtained for the left and right probabilities and the total radiative rate of the lower polariton branch are shown in Fig. 7 in the case of the weak coupling regime discussed in the previous section. Both probabilities are peaked at $k_{\|}=0$. The value at the peak is larger on the air side. This result is expected because of the strong asymmetry of the cavity and of the low number of pairs of the right DBR. At $k_{\|}\simeq 0.8\times 10^5$ cm^{-1} the emission probability in air vanishes, due to the onset of total internal reflection on the air side mirror. For still higher values of $k_{\|}$, light is totally emitted on the substrate side, and the sequence of peaks corresponding to the emission through leaky modes is found. It is clear at this point how leaky modes represent the most important decay channel in MC systems. In fact, the $k_{\|}$ region where leaky modes are found is by far the largest portion of the two-dimensional phase space involved in the decay process. This fact has two important consequences. First, it constitutes the most important limiting factor in the design of light-emitting devices based on semiconductor MC's, where the optimization of the extraction efficiency on the air side is pursued.[39] Furthermore, it strongly influences the polariton dynamics. In fact, the radiative rates corresponding to leaky modes are much larger than the acoustic phonon scattering rate. Consequently, most of the polaritons relaxing inside the radiative zone are emitted through the leaky modes, and only a relatively small fraction of them relaxes to the bottom of the polariton dispersion where they radiate in the normal direction.[35] Thus leaky modes are responsible for a bottleneck effect in the relaxation of excitons from the nonradiative region to polariton states in the radiative region, which takes place in a typical luminescence experiment with nonresonant excitation.

The above calculations allow us to write an expression for the measured luminescence intensity under the hypothesis that the effects of the inhomogeneous broadening mechanisms on the exciton level are negligible. The luminescence spectrum is then simply proportional to a sum of Lorentzian line shapes as follows:

$$I(k_{\|},\omega)\propto\frac{1}{2\pi}\sum_{n=1,2}N_{k_{\|},n}\gamma_{r,k_{\|},n}\frac{\gamma_{k_{\|},n}}{(\omega-\omega_{k_{\|},n})^2+\gamma^2_{k_{\|},n}}, \tag{33}$$

where we have indicated with $N_{n,\mathbf{k}_{\|}}$ the assumed stationary distribution of polariton modes. Expression (33) gives the luminescence spectrum along an arbitrary direction. In addition, using $k_{\|}=(\omega/c)\sin(\theta)$, where θ is the emission angle in air, Eq. (33) provides the intensity pattern of the photoluminescence signal.

As a concluding remark of this section, we want to mention the problem of describing the effect of disorder in these systems. In this work we do not consider the influence of disorder at any level. It is well known that, in QW's, interface roughness and alloy disorder destroy the in-plane translational invariance of the system. In particular, in sufficiently narrow QW's ($L_{\mathrm{QW}}\sim 200$ Å or less), there is experimental evidence for the dominant role of interface roughness in determining the exciton properties.[36] Interface roughness results in a perturbation of the otherwise flat potential governing electron and hole motion along the QW plane. This, in turn, influences both the relative electron-hole motion and the exciton center of mass motion.[36] In particular, the presence of ''islands'' of lateral confining potential along the plane suggests the existence of exciton states with localized center of mass motion. Exciton localization is known to modify the exciton radiative properties in bare QW's.[34] In this case, we can argue that the localized exciton wave function will be characterized by a $k_{\|}$ uncertainty, in contrast with free exciton states. The order of magnitude of this $k_{\|}$ uncertainty is given by the inverse of the size of the confining islands. For good quality samples, this size is of the order of 300 Å, which corresponds to a $\Delta k_{\|}$ of the order of ten times the width of the radiative region. However, in absorption or photoluminescence experiments, the direct evidence of disorder effects is represented by an inhomogeneous *energy* broadening of the exciton line shape. How these two

quantities are related is not, at present, very clear from the existing literature. Moreover, when considering measurements on MC's, the value of $\Delta k_{\parallel}$ estimated above is in contrast with the experimental observations. In fact, Houdré *et al.*[4] have measured the MC polariton dispersion by means of a photoluminescence experiment with nonresonant excitation. This dispersion amounts to a few meV within the radiative region. This is in accord with the results of the present work and confirms the picture of free excitons here adopted. We argue that these two apparently contrasting pieces of evidence can be explained if we suppose that the exciton-photon coupling ''rebuilds'' the in-plane coherence of the localized exciton states lying within the frequency width of the cavity mode. In fact, the photon modes still maintain their translational symmetry inside the MC, independently of the nature of the exciton states. Thus we expect that, when the inhomogeneous energy broadening (the only parameter which allows one to quantify disorder in real samples) is smaller than the nominal Rabi splitting, the phase-coherence loss is slower than the Rabi oscillation and, consequently, the translational invariance of the mixed exciton-photon state is preserved. This condition can be used to extend the definition of very strong coupling regime to include the overall (homogeneous plus inhomogeneous) exciton broadening. We conclude that, in the very strong coupling regime, localization is strongly inhibited because of the strong exciton-photon coupling, and the picture of free excitons is still valid, provided an inhomogeneous energy broadening of the exciton level is included in the calculations. We are currently addressing this problem, which will be the subject of a subsequent publication. Concerning the weak coupling regime, it is clear that in this case the states involved in the luminescence problem are those perturbed by the lateral disordered potential. In this case, the influence of localization on the radiative rates should be described, as in Ref. 34 for bare QW's, by allowing for the modification of the photon density of states due to the cavity.

V. CONCLUSIONS

This paper mainly consists of two parts. In the first part we have presented a quantum theory of QW exciton polaritons in arbitrary semiconductor microcavities. The polariton dispersion relation has been obtained and solved in some representative cases. The dispersion represents the energy position and broadening of the resonances in the polariton density of states. Two coupling regimes are usually distinguished: the weak coupling regime and the strong coupling regime. This model applies equally well to the two cases. We have described the polariton dispersion in two model structures presenting weak and strong coupling behavior at resonance, respectively. Furthermore, by varying the cavity mode confinement, we have shown the behavior of the polariton energy and decay rate in the transition from the weak to the strong coupling regime. The most important aspect of this transition is that the peak in the polariton decay rate appears in the intermediate coupling region. This is significant if we seek for a maximum enhancement of the radiative emission along the normal direction, as required in most vertical emitting structures. A comparison of the present results with existing measurements of the polariton dispersion in the strong coupling case has been made. The data are well reproduced by our calculations if the exact cavity geometry is used. Moreover, no adjustable parameter has been introduced and the known value of the exciton oscillator strength was used.

In the second part of this work we tried to link the results of the theory of microcavity polaritons to experimentally observed quantities, namely, the photoluminescence spectrum. In order to properly characterize the photoluminescence process, it is necessary to identify the lowest excited states from which the luminescence originates, and to define for them a radiative decay rate. We have shown that this identification is unambiguous only in two limiting cases where the polariton resonances can be considered as quasimodes. This happens when the system is in the very strong or very weak coupling regime. In these two cases an expression for the radiative rates has been provided. In addition, these rates have been further subdivided by considering emission into the substrate and into air separately. This finally leads to an expression for the observed photoluminescence intensity as a function of frequency and emission angle. The most important result of this analysis concerns the role of leaky modes of the MC system on the emission process. Leaky modes constitute the dominant decay channel in luminescence experiments performed with nonresonant excitation. This effect is undesirable when trying to improve the performances of light-emitting devices, because radiation through leaky modes is totally dissipated inside the sample substrate. Our model provides the radiative decay rates in the leaky mode region of k space as well as those through the main cavity mode. This result consitutes the first step for a detailed description of the relaxation-emission process, aimed at both a better understanding of the radiative processes peculiar to these structures and an improvement of the performance of modern MC-based light-emitting devices. Finally, we remark that this analysis of the luminescence process gives evidence for the existence of an intermediate region of coupling where the dynamics of the relaxation and of the decay processes cannot be treated separately. In this case a simple description of the luminescence in terms of decay rates of polariton quasimodes becomes impossible and an extension of the present model, which includes relaxation into the whole continuum of polariton states, would be necessary. We have already remarked that the intermediate coupling region is the most interesting for device application. The extension of the model to these cases will thus constitute the leading subject of our future work on microcavities.

ACKNOWLEDGMENTS

We wish to thank L. C. Andreani, R. Houdré, P. Pellandini, S. Savasta, and R. P. Stanley for many useful hints and fruitful discussions. F.T. acknowledges support from the Swiss Optics Priority Program and C.P. from the Swiss National Foundation.

[1] See, e.g., *Confined Electrons and Photons: New Physics and Devices*, edited by E. Burstein and C. Weisbuch (Plenum, New York, 1994).
[2] C. Weisbuch, M. Nishioka, A. Ishikawa, and Y. Arakawa, Phys. Rev. Lett. **69**, 3314 (1992).
[3] H. Yokoyama, K. Nishi, T. Anan, H. Yamada, S. D. Bronson, and E. P. Ippen, Appl. Phys. Lett. **57**, 2814 (1990).
[4] R. Houdré, C. Weisbuch, R. P. Stanley, U. Oesterle, P. Pellandini, and M. Ilegems, Phys. Rev. Lett. **73**, 2043 (1994).
[5] T. A. Fisher, A. M. Afshar, D. M. Whittaker, M. S. Skolnick, J. S. Roberts, G. Hill, and M. A. Pate, Phys. Rev. B **51**, 2600 (1995).
[6] J. Tignon, P. Voisin, C. Delalande, M. Voos, R. Houdré, U. Oesterle, and R. P. Stanley, Phys. Rev. Lett. **74**, 3967 (1995).
[7] T. B. Norris, J. K. Rhee, C. Y. Sung, Y. Arakawa, M. Nishioka, and C. Weisbuch, Phys. Rev. B **50**, 14 663 (1994).
[8] J. Jacobson, S. Pau, Hui Cao, G. Bjork, and Y. Yamamoto, Phys. Rev. A **51**, 2542 (1995).
[9] Y. Yamamoto, S. Machida, K. Igeta, and G. Bjork, in *Coherence, Amplification, and Quantum Effects in Semiconductor Laser*, edited by Y. Yamamoto (Wiley, New York, 1991), p. 561.
[10] G. Bjork, S. Machida, Y. Yamamoto, and K. Igeta, Phys. Rev. A **44**, 669 (1991).
[11] C. Cohen-Tannoudji, J. Dupont-Roc, and G. Grynberg, *Processus d'Interaction entre Photons et Atomes* (Editions du CNRS, Paris, 1988).
[12] J. J. Hopfield, Phys. Rev. **112**, 1555 (1958).
[13] V. M. Agranovich and A. O. Dubowskii, Pis'ma Zh. Éksp. Teor. Fiz. **3**, 345 (1966) [JETP Lett. **3**, 233 (1966)].
[14] L. C. Andreani and F. Bassani, Phys. Rev. B **41**, 7536 (1990).
[15] V. Savona, Z. Hradil, P. Schwendimann, and A. Quattropani, Phys. Rev. B **49**, 8774 (1994).
[16] P. Meystre, Prog. Opt. **30**, 261 (1992).
[17] H. J. Carmichael, R. J. Brecha, M. G. Raizen, H. J. Kimble, and P. R. Rice, Phys. Rev. A **40**, 5516 (1989).
[18] V. Savona, L. C. Andreani, P. Schwendimann, and A. Quattropani, Solid State Commun. **93**, 733 (1995).
[19] Y. Chen, A. Tredicucci, and F. Bassani, Phys. Rev. B **52**, 1800 (1995).
[20] V. Savona and F. Tassone, Solid State Commun. **95**, 673 (1995).
[21] D. S. Citrin, IEEE J. Quantum Electron. **30**, 997 (1994).
[22] S. Jorda, Phys. Rev. B **50**, 18 960 (1994).
[23] S. Jorda, Phys. Rev. B **51**, 10 185 (1995).
[24] H. A. McLeod, *Thin-Film Optical Filters*, 2nd ed. (Hilger, Bristol, 1986).
[25] S. Jorda, Phys. Rev. B **50**, 2283 (1994).
[26] See, e.g., L. C. Andreani, in *Confined Electrons and Photons: New Physics and Devices* (Ref. 1).
[27] P. M. Morse and H. Feshbach, *Methods of Theoretical Physics* (McGraw-Hill, New York, 1953), Pt. I, Chap. 7.
[28] Z. Hradil, A. Quattropani, V. Savona, and P. Schwendimann, J. Stat. Phys. **76**, 299 (1994).
[29] F. Tassone, F. Bassani, and L. C. Andreani, Nuovo Cimento D **12**, 1673 (1990).
[30] D. S. Citrin, Phys. Rev. B **49**, 1943 (1994).
[31] B. Zhang, S. S. Kano, Y. Shiraki, and R. Ito, Phys. Rev. B **50**, 7499 (1994).
[32] R. Houdre (private communication).
[33] C. Piermarocchi, F. Tassone, V. Savona, P. Schwendimann, and A. Quattropani, in Proceedings of the 4th Conference on the Optics of Excitons in Confined Structures, Cortona, 1995 [Nuovo Cimento D **17**, 184 (1995)].
[34] D. S. Citrin, Phys. Rev. B **47**, 3832 (1993).
[35] F. Tassone, C. Piermarocchi, V. Savona, P. Schwendimann, and A. Quattropani, in *Proceedings of a NATO Advanced Research Workshop on Quantum Optics in Wavelength Scale Structures*, edited by J. G. Rarity and C. Weisbuch (Plenum Press, New York, in press); Phys. Rev. B **53**, R7642 (1996).
[36] J. Hegarty, L. Goldner, and M. D. Sturge, Phys. Rev. B **30**, 7346 (1984).
[37] L. C. Andreani, V. Savona, P. Schwendimann, and A. Quattropani, Superlatt. Microstruct. **15**, 453 (1994).
[38] More precisely, two approximations are introduced in order to obtain (27) from (25). The first one consists in calculating only the residua of the integrand which correspond to the two main polariton poles, neglecting all those deriving from the other DBR resonances outside the stop band. These latter have negligible contributions for values of ω close to the main cavity mode. The second approximation is the *polariton pole approximation*, which consists in replacing $\Sigma^{(\mathrm{ret})}_{\mathbf{k}_\parallel}(E)$ with $\Sigma^{(\mathrm{ret})}_{\mathbf{k}_\parallel}(\hbar(\omega_{k_\parallel,n}-i\gamma_{k_\parallel,n}))$ in the two pole contributions to the Green's function in the integrand of (25).
[39] H. De Neve, J. Blondelle, R. Baets, P. Demeester, P. Van Daele, and G. Borghs, IEEE Photon Technol. Lett. **7**, 287 (1995).